PALAIOS
Emphasizing the impact of life on Earth's history

PALAIOS, 2019, v. 34, 437–451
Research Article
DOI: http://dx.doi.org/10.2110/palo.2019.030

EXPERIMENTAL PRESERVATION OF MUSCLE TISSUE IN QUARTZ SAND AND KAOLINITE

SHARON A. NEWMAN,[1,2] MIRNA DAYE,[1] SIRINE C. FAKRA,[3] MATTHEW A. MARCUS,[3] MIHKEL PAJUSALU,[1] SARA B. PRUSS,[4] EMILY F. SMITH,[5] AND TANJA BOSAK[1]

[1]*Department of Earth, Atmospheric and Planetary Sciences, Massachusetts Institute of Technology, Cambridge, Massachusetts 02139, USA*
[2]*Division of Geological and Planetary Sciences, California Institute of Technology, Pasadena, California 91125, USA*
[3]*Advanced Light Source, Lawrence Berkeley National Laboratory, Berkeley, California 94720, USA*
[4]*Department of Geosciences, Smith College, Northampton, Massachusetts 01063, USA*
[5]*Department of Earth and Planetary Sciences, Johns Hopkins University, Baltimore, Maryland 21218, USA*
email: snewman@caltech.edu

ABSTRACT: **Siliciclastic sediments of the Ediacaran Period contain exceptionally preserved fossils of macroscopic organisms, including three-dimensional casts and molds commonly found in sandstones and siltstones and some two-dimensional compressions reported in shales. The sporadic and variable associations of these exceptionally preserved macroscopic fossils with pyrite, clay minerals, and microbial fossils and textures complicate our understanding of fossilization processes. This hinders inferences about the evolutionary histories, tissue types, original morphologies, and lifestyles of the enigmatic Ediacara biota. Here, we investigate the delayed decay of scallop muscles buried in quartz sand or kaolinite for 45 days. This process occurs in the presence of microbial activity in mixed redox environments, but in the absence of thick, sealing microbial mats. Microbial processes that mediate organic decay and release the highest concentrations of silica and Fe(II) into the pore fluids are associated with the most extensive tissue decay. Delayed decay and the preservation of thick muscles in sand are associated with less intense microbial iron reduction and the precipitation of iron oxides and iron sulfides that contain Fe(II) or Fe(III). In contrast, muscles buried in kaolinite are coated only by <10 µm-thick clay veneers composed of kaolinite grains and newly formed K- and Fe(II)-rich aluminosilicate phases. Muscles that undergo delayed decay in kaolinite lose more mass relative to the muscles buried in sand and undergo vertical collapse. These findings show that the composition of minerals that coat or precipitate within the tissues and the vertical dimension of the preserved features can depend on the type of sediment that buries the muscles. Similar processes in the zone of oscillating redox likely facilitated the formation of exceptionally preserved macrofossils in Ediacaran siliciclastic sediments.**

INTRODUCTION

Ediacaran macroscopic organisms were commonly preserved in globally distributed siliciclastic sediments as three-dimensional casts and molds (Gehling 1999; Narbonne 2005; Callow and Brasier 2009) and two-dimensional compression fossils (Zhu et al. 2008; Cai et al. 2010, 2012; Anderson et al. 2011). Because these organisms were likely composed of easily degradable, labile tissues (Fedonkin and Waggoner 1997; Meyer et al. 2014b), their common and exceptional preservation in siliciclastic sediments requires explanation. Various environmental and biological factors have been hypothesized (Gehling 1999; Narbonne 2005; Callow and Brasier 2009; Laflamme et al. 2011; Darroch et al. 2016; Liu 2016; Tarhan et al. 2016) and many of these interpretations remain to be tested experimentally and/or confirmed from geological observations. Moreover, the preservation potential of labile tissues in the absence of cuticles or other external hard features remains poorly constrained. If improved, models of Ediacaran preservation would enable better reconstructions of the taxonomic affiliations, evolutionary histories, and lifestyles of Ediacaran organisms (Xiao and Laflamme 2009; Erwin et al. 2011).

The fossils of Ediacaran soft-bodied organisms are commonly associated with pyrite or iron oxides (e.g., Borkow and Babcock 2003; Cai et al. 2012; Meyer et al. 2014a; Schiffbauer et al. 2014; Liu 2016; Smith et al. 2016, 2017; Liu et al. 2019). Iron sulfides are hypothesized to precipitate on and/or around labile tissues during early diagenesis due to the microbial reduction of sulfate and Fe(III) and the adsorption of Fe(II) ions onto tissues in a process similar to tanning (Berner 1969; Petrovich 2001). The replacement of organic material by pyrite minerals is a common mode of preservation in late Ediacaran and early Phanerozoic sediments, but is rarely associated with the formation of Ediacaran casts and molds (e.g., Cai et al. 2011, 2012; Smith et al. 2017). A second model of preservation, proposed by Gehling (1999) and inspired by the common association of exceptionally preserved microbial textures with the fossils of Ediacaran organisms, invokes the role of photosynthetic microbes in the formation of pyrite sole veneers. In this model, photosynthetic microbial mats colonize the sand that buries Ediacaran organisms, thereby sealing tissues in anoxic environments beneath the sediment surface and concentrating ions necessary for the precipitation of pyrite cements (Gehling 1999). This model is consistent with the occurrence of red stains on the soles of fossiliferous event beds due to the cementation of sand grains by iron oxides, interpreted by Liu et al. (2019; see also Gehling and Vickers-Rich 2007) to be products of pyrite oxidation. However, to date, direct evidence for the association of pyrite (or early oxide) cementation with cast-and-mold fossils has not been found. Moreover, Tarhan et al. (2015, 2018) suggest that iron oxides in the Ediacara Member of the Rawnsley Quartzite of South Australia likely originated from recent groundwater activity, bringing into question the role of pyrite in early preservation processes.

Published Online: September 2019
 0883-1351/19/034-437

Taphonomic experiments can shed additional light on the role of pyrite in the preservation of non-mineralizing organisms. Elemental enrichments of iron and sulfur were detected around decaying lepidopteran larvae (Darroch et al. 2012), sea anemones, and mollusks (Gibson et al. 2018) after weeks of burial beneath layers of fine-grained sand. Darroch et al. (2012) observed these elemental enrichments associated with soft tissue surfaces and Gibson et al. (2018) observed enrichments in the sediments directly adjacent to decaying tissues. Iron sulfide mineral phases have also been experimentally formed on and within decaying plant material (Grimes et al. 2001; Brock et al. 2006). These experiments suggest that iron and sulfur-bearing minerals likely play a role in the preservation of organics, but the detection of pyrite or other iron sulfide minerals on labile animal tissues by methods of X-ray diffraction or other phase identification techniques has not been previously reported.

The presence of non-pyritized fossils in the Ediacaran and early Cambrian fossil record further complicates our understanding of the importance of pyritization in the preservation of soft-bodied organisms. Pyritized casts and molds, such as those of *Gaojiashania* and *Conotubus* (e.g., Smith et al. 2017), commonly occur in the same event beds with other fossils that lack pyrite (Schiffbauer et al. 2014; Smith et al. 2016) and many Ediacaran assemblages do not contain evidence of pyrite associated with fossils (e.g., Tarhan et al. 2016). Moreover, well-preserved Ediacaran fossils are associated with diverse minerals, including calcite (e.g., Bykova et al. 2017), clays (e.g., Gehling 1999), and silica (e.g., Tarhan et al. 2016). Inspired by evidence of silica cementation in the fossiliferous assemblages of the Ediacara Member of South Australia, Tarhan et al. (2016) proposed a model for preservation that requires the rapid precipitation of silica cements around soft tissues, due to the elevated concentrations of dissolved silica in Precambrian seawater. In contrast, using evidence from the White Sea Region in Russia, Bobrovskiy et al. (2019) suggest that differences in the mechanical properties of the sediments overlying and underlying decaying soft tissues affect fluid flow through the system and facilitate fossil preservation.

The common occurrence of clay laminae between part-counterpart impressions (Gehling 1999), clay minerals in the veins (Meyer et al. 2014a) and upper/lower margins (Laflamme et al. 2011) of fossils, and the formation of two-dimensional compression fossils in clay-rich shales (Cai et al. 2012) have also inspired hypotheses about the role of clay minerals in preservation processes. Previous empirical studies have shown that clay minerals facilitate the delayed decay of non-mineralizing organisms (Wilson and Butterfield 2014; Naimark et al. 2016a, 2016b, 2018a, 2018b). Naimark et al. (2016a) and Wilson and Butterfield (2014) reported better preservation of arthropods in the presence of kaolinite (a 1:1 clay) relative to montmorillonite (a 2:1 clay), calcite, or quartz. An experimental study demonstrated that kaolinite can inhibit the growth of an aerobic heterotrophic microbe, *Pseudomonas luteoviolacea* (McMahon et al. 2016). Clay minerals around fossils can have multiple origins, including the background sediment and authigenic precipitation (e.g., Wacey et al. 2014). Photosynthetic microbes have been experimentally shown to trap fine-grained minerals from sediments and facilitate the precipitation of authigenic clays (Newman et al. 2016, 2017). These processes can preserve the shapes of microbial cells, mats, and leaves (Newman et al. 2016, 2017; Locatelli et al. 2017). The similarity between sediment trapping in microbial systems (Newman et al. 2016, 2017) and the adhesion of fine-grained particles to invertebrate eggs (Martin et al. 2004) suggests that clay minerals may also physically protect labile animal tissues from degradation by heterotrophic microbes.

The current study uses experimental taphonomy to probe the roles of quartz-rich sand, kaolinite, illite, and microbial metabolisms in the preservation of scallop adductor muscles. These were selected as model tissues because they are readily available and are similar to some Ediacaran organisms in size (~5 cm), discoidal morphology, and likely, proteinaceous composition (Dzik 1999). Our focus on kaolinite was inspired by previous decay experiments (e.g., Wilson and Butterfield 2014; Naimark et al. 2016a, 2016b) and because kaolinite is an abundant component of the clay fraction of some modern marine sediments (Griffin et al. 1968). Illite was also selected because this clay has been previously shown to encrust cyanobacterial filaments (Newman et al. 2016, 2017) and has been reported as a mineral phase associated with microfossils in ~1 Ga lake sediments (Wacey et al. 2014). Our study expands on previous experimental work (e.g., Darroch et al. 2012; Wilson and Butterfield 2014; Naimark et al. 2016a, 2016b, 2018a, 2018b) by enabling a more active transport of ions and solutes and by characterizing the preservation of organisms that lack resistant cuticles. This better mimics tidal pumping and solute exchange (Bosak et al. 2013; Newman et al. 2017) in subtidal and intertidal marine environments where many late Ediacaran assemblages are reported (e.g., Gehling 1999; Arrouy et al. 2016; Elliott et al. 2016; Smith et al. 2016, 2017), as well as the hypothesized tissue composition of most Ediacaran organisms. This study demonstrates the effects of sediment grain size and composition on the preservation of soft tissues and contributes to our understanding of how environmental and biological factors can facilitate differing mechanisms of fossilization.

MATERIALS AND METHODS

Soft Tissue Preparation

To identify factors that determine the preservation of labile animal tissues in siliciclastic environments, we incubated scallop adductor muscles in quartz sand or kaolinite (Fig. 1). Fresh, untreated Atlantic sea scallops (*Placopecten magellanicus*) were purchased from the New Deal Fish Market (Cambridge, MA, USA). The adductor muscles were cut from the shells and frozen at -20°C for one to two days to prevent the decay of tissues before incubation. On the first day of the experiment, muscles were thawed at room temperature, rinsed with double distilled water to remove dirt, sand, and other impurities and sterilized by soaking in 100% 200-proof ethanol for 20 min. This procedure sterilized the surface of the muscles, but did not sterilize all endogenous bacteria. The ethanol was decanted by pouring and the muscles were left in the fume hood for one hour to evaporate excess ethanol. Any remaining ethanol was removed by rinsing the muscles three times with filter-sterilized double distilled water (0.2 μm Nalgene Rapid Flow Sterile Top Filters, VWR, Radnor, PA, USA). Muscles were weighed directly after rinsing and before incubation.

We also conducted preliminary experiments that compared the decay of muscle tissues that were frozen and sterilized with ethanol before experimentation and those that were incubated immediately after removal from the shell. No differences were observed between these experiments. Therefore, all experiments presented here used muscles that had been frozen and ethanol-sterilized before incubation to focus on the role of endogenous bacteria in soft tissue decay and eliminate decay due to surficial contaminants that were introduced after the removal of scallops from their natural habitat.

Muscles Buried in Sand in the Presence of Cyanobacteria or Illite

To investigate the decay of soft tissues buried in siliciclastic sand, muscles were incubated in 68 mm tall and wide sterile culture jars (Grenier Bio-One, Kremsmünster, Austria) in the presence of 130 g of quartz sand (Ottawa Silica Company, Ottawa, IL, USA). The sand contained quartz, mica, and iron oxides. Cation-rich aluminosilicates made up 0.03 weight percent of the sand (see Newman et al. 2017). The sand was sterilized before experimentation by autoclaving at 121°C for 20 min. Cyanobacterial inoculums (see Newman et al. 2017 for a description of the microbial community composition) (Fig. 1A, Table 1) or cm-thick layers of illite (Time Laboratories, Pocatello, ID, USA) (Fig. 1B, Table 1) were added to the experiments to investigate the roles of photosynthetic microbes and illite on muscle preservation, respectively. Cyanobacteria were inoculated

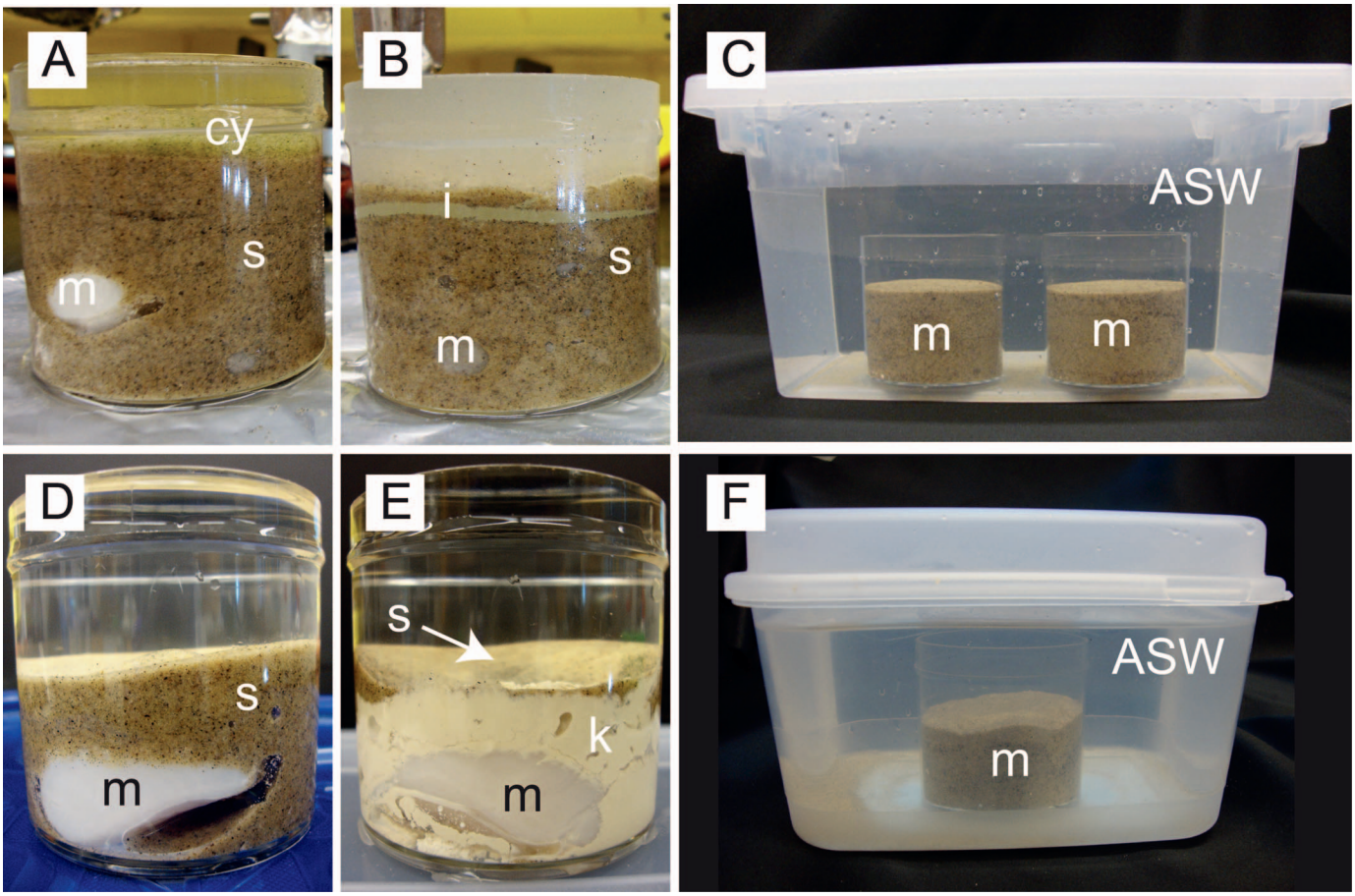

FIG. 1.—Photographs of taphonomy experiments. **A**) Muscle is incubated in quartz sand in the presence of cyanobacteria. **B**) Muscle is incubated in quartz sand in the presence of a cm-thick layer of illite. **C**) Two replicate culture jars are incubated in 2 L of artificial seawater. **D**) Muscle is incubated in quartz sand without added clays or microbes. **E**) Muscle is incubated in 30 g of kaolinite and covered by a ~1.5 cm-thick layer of sand. **F**) A single culture jar is incubated in 1.5 L of artificial seawater. Culture jar volume is 190 mL. Abbreviations: m = muscle; s = sand; cy = cyanobacteria; i = illite; ASW = artificial seawater medium; k = kaolinite.

onto the surface of the sand in 10 mL of artificial seawater using a plastic serological pipette. These microbes were inoculated several times during the muscle burial experiment to facilitate the formation of cyanobacterial mats.

Two replicate culture jars, each containing a single muscle buried in sand, were placed in a larger plastic container (26.5 × 15.5 × 14.0 cm [l × w × h], Sterilite Medium Clip Box, Sterilite Corporation, Townsend, MA, USA) that had been pre-filled with 2 L of artificial seawater (Fig. 1C). This sterile medium contained 1.1 μM Fe(III) (iron (III) hexachloride), as well as low concentrations of sulfate (5.0 mM) and similar concentrations of dissolved silica (0.1 mM) relative to modern ocean values (Pilson 2013). Newman et al. (2016, table dr1) and Newman et al. (2017, table s1) describe the composition of the medium in greater detail. Control experiments investigated muscles buried in sand in the absence of cyanobacteria and added illite (Fig. 1D). All experiments were conducted in triplicate and included a total of 18 muscles buried in sand: six muscles incubated in the presence of cyanobacteria, six muscles incubated in the presence of sterile illite, and six muscles incubated in the control experiments (see Table 1 for a list of all experiments). After 30 and 45 days of burial, muscles were exhumed from the sand with a sterile serological pipette with a gentle lifting motion. Wet muscles were exhumed from the sand, rinsed three times with double distilled water, and weighed immediately after rinsing to determine the loss of mass due to decay.

Muscles Buried in Kaolinite

Muscles were covered by 30 g of kaolinite (Santa Cruz Biotechnology, Inc., Dallas, TX, USA) in sterile jars (Fig. 1E, Table 1). Kaolinite was sterilized before experimentation by autoclaving at 121°C for 20 min. Muscles were buried a few cm below the kaolinite surface and a ~1.5 cm-thick layer of sterile sand was added to the surface of the sediment to prevent the suspension of kaolinite into the solution in the continuously agitated jars (Fig. 1E). Control conditions investigated the decay of muscle tissues buried in sterile sand (130 g) without added kaolinite under identical conditions to those described above (Fig. 1D). In each control experiment, an additional 1.5 cm-thick layer of sand was added to the top of the substrate to mimic experiments with kaolinite and to maintain the same sediment weight above all muscles. Individual culture jars that contained a single muscle were placed into a larger plastic container with a lid (18.7 × 16.5 × 11.4 cm [l × w × h], Sterilite Flip Top, Sterilite Corporation, Townsend, MA, USA) (Fig. 1F); each large container was pre-filled with 1.5 L of the sterile artificial seawater described above. Both kaolinite and sand experiments were conducted in triplicate and included a total of six muscles: three muscles buried in kaolinite and another three muscles buried in sand (Table 1). Muscles were exhumed on day 45 as described above.

Additional sterile control experiments investigated changes in the water chemistry of the kaolinite/quartz sand substrates in the absence of added muscles. These experiments were identical to those described above, but

TABLE 1.—*Loss of muscle mass after 30 and 45 days of burial and carbon-hydrogen-nitrogen (CHN) content for replicate experiments.*

			Loss of muscle mass (% of original tissue decayed) and CHN content (%)					
			Day 30			Day 45		
Substrate	Cyanobacteria added	ASW (L)**	R1	R2	R3	R1	R2	R3
before burial*	–	–	n.e.	n.e.	n.e.	n.e. C: 40.3 ± 0.6 H: 7.4 ± 0.2 N: 11.1 ± 0.3	n.e. C: 41.1 ± 0.2 H: 7.5 ± 0.1 N: 11.7 ± 0.4	n.e.
sand only	N	2.0	21.6	71.7	100	50.0	100	100
sand only	Y	2.0	100	16.3	95.3	99.0	33.0	100
sand and illite	N	2.0	97.1	17.6	100	100	36.1	100
sand only	N	1.5	n.e.	n.e.	n.e.	100	29.7 C: 48.4 ± 0.8 H: 7.1 ± 0.6 N: 11.0 ± 0.7	100
kaolinite and sand	N	1.5	n.e.	n.e.	n.e.	72.5 C: 44.0 ± 2.2 H: 7.0 ± 0.1 N: 9.1 ± 0.1	60.8 C: 43.5 ± 0.3 H: 6.9 ± 0.1 N: 9.6 ± 0.2	100

Note: R1-R3 denote the three replicate experiments; *n.e.* indicates that no exhumation of muscle tissue was attempted. Values for CHN are below corresponding values for loss of mass; not all replicates were analyzed for CHN content. %CHN are reported as sample averages, measured independently and standard deviation from the mean is also given.

* Muscle was not buried in sand or kaolinite.

** Volume of artificial seawater medium (ASW) before and after weekly medium replacements.

lacked soft tissues buried in kaolinite or sand and remained sterile throughout the 45-day incubation interval.

Analyses of the Exhumed Muscles

Carbon-hydrogen-nitrogen analyses of two muscles before incubation, two exhumed from kaolinite after 45 days, and one exhumed from quartz sand after 45 days were conducted at Micro-Analysis Inc. (Wilmington, DE, USA), using a Perkin Elmer 2400 Series II elemental analyzer (Waltham, MA, USA) (see Online Supplemental File methods for additional details). Statistical analyses were performed using the software package R (version 3.4.4).

To identify the composition and distribution of minerals coating soft tissues, pieces of exhumed muscle (<1 cm) were imaged by scanning electron (SEM) and transmission electron (TEM) microscopy. Samples for SEM were fixed in 2.5% glutaraldehyde in 0.1 M sodium cacodylate buffer, coated with gold and palladium, and imaged on a Zeiss Supra Scanning Electron Microscope with electron-dispersive spectroscopy (Center for Nanoscale Systems, Harvard University, Cambridge, MA, USA). Selected muscle samples were also imaged with a JEOL 2010F transmission electron microscope (TEM, JEOL 2010F, JEOL, CA, USA) with a high-angle annular dark-field detector (HAADF, Gatan, CA, USA) and energy dispersive spectrometer (Bruker silicon drift detector SDD, Bruker, MA, USA). See Online Supplemental File methods for additional details.

The spatial distribution and speciation of iron in exhumed muscles was characterized at the Advanced Light Source beamline 10.3.2 (Marcus et al. 2004) (Lawrence Berkeley National Laboratory, Berkeley, CA, USA), using micro-focused X-ray fluorescence (μXRF) mapping and iron K-edge X-ray absorption near edge structure (μXANES) spectroscopy, respectively (see Online Supplemental File methods). Mineral groups (e.g., silicates, oxides, sulfates, sulfides, etc.) of minerals coating or embedding tissue surfaces were determined by least square combination fitting of XANES spectra with a large iron-bearing standard database from the ALS beamline 10.3.2. All identifications made with this method are tentative. High resolution imaging (TEM; see above) was used to independently confirm mineral group identifications, as well as to identify mineral phases.

Characterization of the Overlying Medium and Pore Fluids

In all experiments, the surface of the artificial seawater medium was in contact with the atmosphere because the plastic containers were not air-tight. Culture jars were continuously agitated on VWR Minishakers (VWR International, Radnor, PA, USA) to facilitate fluid motion; see Newman et al. (2017, their supplementary methods and table S2) for a description of the fluid flow through sediments in the same system. The medium was replaced every 5 to 10 days to remove dissolved organic matter and to maintain a semi-constant pH of ~7.6 in the water column. Pore fluids were sampled from sediments adjacent to the bottom of the decaying muscle tissues (where the top and bottom of the muscle was dictated by its placement in the culture jar) using sterile syringes and needles (VWR, Radnor, PA, USA). In the case of sterile control experiments that did not contain any tissues, pore fluids were sampled ~6.5 cm below the surface of the sediment. Porewaters were then filtered aerobically through 0.2 μm sterile syringe filters with polyethersulfone membranes (Acrodisc®, Pall Laboratory, Westborough, MA, USA). Colorimetric measurements of Fe(II), Fe(III), dissolved silica, and sulfide in filtered porewater samples were made using a Biotek multiplate reader (Synergy 2, Winooski, VT, USA) at the following wavelengths: 562 (iron), 810 (silica), and 670 (sulfide) nm (see Online Supplemental File methods). These measurements tracked changes in solution chemistry associated with organic decay. The pH of the water column was measured with a WTW portable pH meter (Weilheim, Germany). Due to the small volume of extractable pore fluids (<3 mL), the pH of the porewater was measured using colorPHast pH strips (EDM Millipore, Burlington, MA, USA), unless otherwise stated. Saturation indices of various mineral and non-mineral phases were calculated using the computer program PHREEQC Version 1.6 and the measurements of pore fluid composition 15 days after muscle burial. We did not measure aluminum concentrations of the porewaters and saturation

values for clay minerals were calculated with an assumed value of 0.1 μM (Mackin and Aller 1986).

RESULTS

Observations During Muscle Burial and Exhumation

To identify factors that facilitate or inhibit decay, nine muscles were buried in quartz sand without added cyanobacteria or clay minerals, six additional muscles were buried in sand in the presence of cyanobacteria, six muscles were buried in sand in the presence of illite, and three muscles were buried in kaolinite for up to 45 days (Table 1). The surface of the artificial seawater medium was in constant contact with the atmosphere, but due to organic decay during the first two weeks of incubation, the concentrations of dissolved oxygen in the pore fluids decreased to less than four μM in all experiments (see Online Supplemental File methods and results, Fig. S1) (Pajusalu et al. 2018). The overlying solution became cloudy (Fig. 2, Online Supplemental File Fig. 2) and malodorous due to the release of degraded organic matter into the water column. Dark gray to black patches formed around some muscles buried in sandy substrates during the first 15 to 30 days of burial (Fig. 2, Online Supplemental File Fig. 2), expanding with time around samples that underwent complete decay. In contrast, visible dark patches did not form around muscles that were exhumable on day 45 (Fig. 2, Online Supplemental File Fig. 2). Thus, the formation of dark patches was an indicator of extensive anaerobic heterotrophic activity and conditions that were not conducive to preservation.

When muscles were buried in kaolinite, mm-thick gray patches appeared around all tissues during the first 15 days of incubation (Fig. 2C, 2D). However, these lighter patches did not predict the extent of decay on day 45. The sand and clay substrates in control experiments that lacked soft tissues did not change color, indicating that these environments remained sterile throughout the 45-day incubation interval.

Wet muscles were weighed before burial and after exhumation to quantify decay. After 30 days, muscles lost 16–100% of the initial mass and two out of three specimens were exhumed from each set of replicate experiments that contained sand only, sand with cyanobacteria, and sand with illite (Table 1, Online Supplemental File Fig. 2A–2C). Muscles exhumed from all substrates on day 45 lost 30–100% of their original mass (Table 1). Only one of the three replicate muscles was exhumed from all sandy substrates and two of the three were exhumed from kaolinite (Fig. 2, Table 1, Online Supplemental File Fig. 2D–2F) after 45 days. Muscles that were not exhumable had liquefied or decayed into mm-sized pieces due to heterotrophic microbial activity (Table 1, Online Supplemental File Fig. 2). The measured loss of mass was consistent with the chemical evolution of the solution (see below) as well as with the visual observations of the continued release of organic material that clouded the overlying medium after each weekly medium replacement.

The loss of mass and changes in the appearance of muscle fibers attested to the decay of all buried muscles (Fig. 2, Table 1, Online Supplemental File Fig. 2). Scanning electron micrographs (SEMs) of fresh muscles revealed intact muscle fibers that were distributed as parallel bands and surrounded by connective tissues (Fig. 3A). In contrast, muscles exhumed on day 45 had lost this banding, indicating extensive decay (Fig. 3B–3F). We did not observe any differences in the morphology of replicate samples collected on days 30 and 45.

CHN Analyses

Carbon-hydrogen-nitrogen (CHN) analyses of fresh muscle tissues and those exhumed from kaolinite revealed a higher carbon content in exhumed tissues (%C: muscle incubated in kaolinite = 43.8% ± 1.5; fresh muscle = 40.7% ± 0.6; t-test with Bonferroni correction, $t = 4.8$, $df = 7$, $p < 0.01$) (Table 1). The opposite trend was observed for both hydrogen and nitrogen; muscles had lower hydrogen and nitrogen contents after 45 days of incubation in kaolinite relative to those that had not undergone incubation (%H: muscle incubated in kaolinite = 7.0 ± 0.1; fresh muscle = 7.5 ± 0.2; t-test with Bonferroni correction, $t = -7.0$, $df = 9$, $p < 0.01$) (%N: muscle incubated in kaolinite = 9.4% ± 0.3; fresh muscle = 11.4 ± 0.5; t-test with Bonferroni correction, $t = -9.2$, $df = 8$, $p < 0.01$) (Table 1). A single muscle exhumed from quartz sand was analyzed and had carbon, hydrogen, and nitrogen contents of 48.4% ± 0.8, 7.06% ± 0.6, and 11.03% ± 0.7, respectively (Table 1). This was similar to the CHN content of muscles exhumed from kaolinite, but with higher nitrogen content. Taken together, this demonstrated that proteins and other nitrogenous compounds were preferentially degraded when muscles were buried in kaolinite.

Muscles Exhumed from Quartz Sand

Muscles recovered from quartz sand maintained their vertical thickness throughout burial and exhumation. These muscles also returned to the original shape after compression by tweezers. However, minerals were not visible on the surfaces (Fig. 2A, Online Supplemental File Fig. 2).

X-ray Absorption Near Edge Structure (XANES) spectroscopy of three muscles exhumed from sand on day 30 and three muscles exhumed from sand on day 45 indicated the accumulation of iron in the tissues and the presence of phases that contained both Fe(II) and Fe(III) (Fig. 4, Online Supplemental File Fig. 3a, Table 1). Least square combination fitting of XANES spectra with iron-bearing standards from the 10.3.2 database (see Online Supplemental File methods) suggested the presence of Fe(II) sulfates and sulfides, as well as iron oxides in muscle tissues (Online Supplemental File Fig. 3a, Table 1). Because pore fluids were consistently undersaturated with respect to iron sulfate precipitation (Table 2), these results likely do not reflect the presence of sulfate minerals around muscles, but may indicate the presence of an amorphous iron sulfate phase. All mineral groups were confirmed and mineral phases were identified by TEM (see Methods and Online Supplemental File methods). The TEM-SAED patterns and d-spacing of minerals embedded in these muscles were consistent with the presence of greigite and hematite (Fig. 5). The iron-rich minerals, which were less than 5 μm wide (Fig. 5C), likely penetrated into the tissue surface, but the extent of impregnation could not be determined by the current method. Clay minerals were rarely detected on muscles that were buried in sediments without added kaolinite or illite (Online Supplemental File Table 1).

Cyanobacteria were inoculated onto the surface of sand in some experimental replicates (Fig. 1A, Table 1) to test whether cyanobacterial mats can delay the decay of muscle tissues in sand. After five days, microbial mats began to form on the surface of the sediment, but by day 15, these aggregates had completely detached from the surface of the substrate and lost their green pigment (Online Supplemental File Fig. 2A, 2D). A continuous mat never formed despite repeated inoculations, indicating that conditions for cyanobacterial growth were not optimal. This was due to the low porewater pH (4.5 to 7.5 in all experiments) (Online Supplemental File tables 2, 3), organic-rich and opaque water column (Online Supplemental File Fig. 2A, 2D), and anoxic conditions (see Online Supplemental File results, Fig. 1). In all experiments that contained sand, only one out of three muscles was exhumable on day 45 (Table 1, Online Supplemental File Fig. 2) and minerals coating muscles did not differ between experiments with and without cyanobacteria. Thus, the delayed decay of muscle tissues did not appear to require the presence of cyanobacteria in the overlying sediment.

Muscles Exhumed from Clay-Rich Substrates

Muscles exhumed from kaolinite after 45 days were covered by dark, rigid veneers that were visible to the naked eye (Fig. 2C). Tissues encrusted by these veneers were vertically compressed due to the weight of the overlying sediment, but maintained their discoidal shape during exhuma-

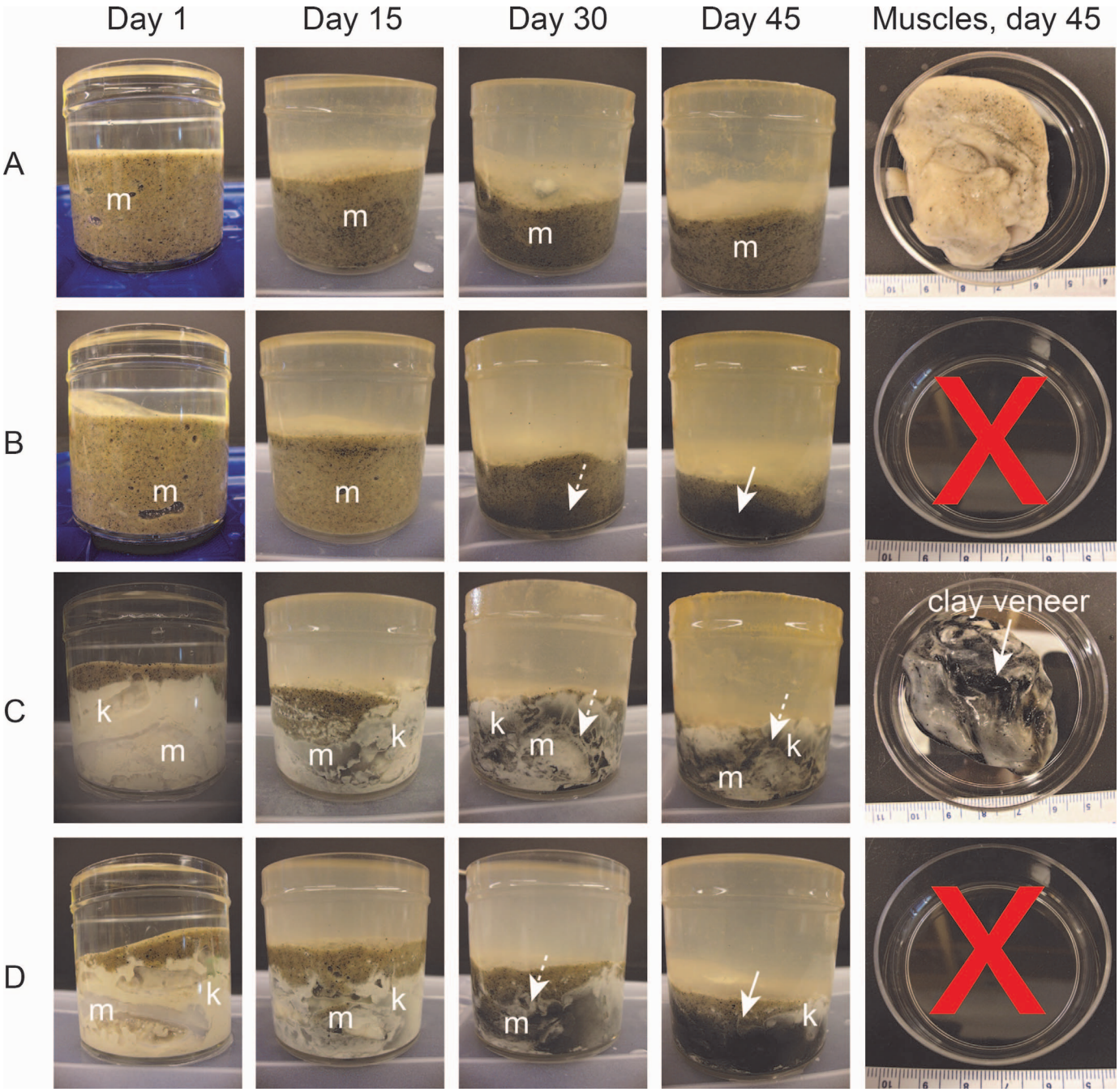

FIG. 2.—Photographs of decaying muscles on days 1, 15, 30, and 45 and specimens exhumed on day 45. Rows represent different experiments and the first four columns reveal progressively advanced time points. Specimens exhumed on day 45 are shown in the rightmost column. **A**) Muscle buried in quartz sand that was exhumed on day 45. **B**) Replicate muscle buried in quartz sand that completely decayed by day 45. **C**) Muscle buried in kaolinite that was exhumed on day 45. **D**) Replicate muscle buried in kaolinite that completely decayed by day 45. Solid arrows point to extensive black patches around muscles that are indicative of heterotrophic microbial activity; dashed arrows point to less extensive, gray patches in kaolinite. Abbreviations: m = muscle; k = kaolinite; X = the complete decay of muscle tissue.

tion and later treatments. Most attempts to separate the veneers from the underlying muscles were unsuccessful. In rare instances when we were able to remove pieces of the coatings, the organic interiors of the samples immediately liquefied, indicating that the veneers provided physical support to the decaying tissues.

SEM-EDS indicated the presence of aluminosilicates on tissue surfaces (Fig. 3), but Fe-rich minerals were only detected by higher resolution (TEM) imaging and the more sensitive synchrotron-based spectroscopic analyses. These minerals were either morphologically indistinguishable from the tissues (Fig. 3E) or occurred as platy grains embedded into the muscle surfaces (Fig. 3F). XANES spectra were consistent with Fe(II) bearing clay mineral standards and kaolinite grains (Online Supplemental File Fig. 3, Table 1). TEM-EDS analyses of these minerals demonstrated the presence of K, Al, Si, and Fe (Fig. 5); their diffraction pattern and d-spacing matched with beidellite (a smectite; Brindley and Semples 1977). The absence of Fe- and K-rich clay minerals from both the sterile kaolinite

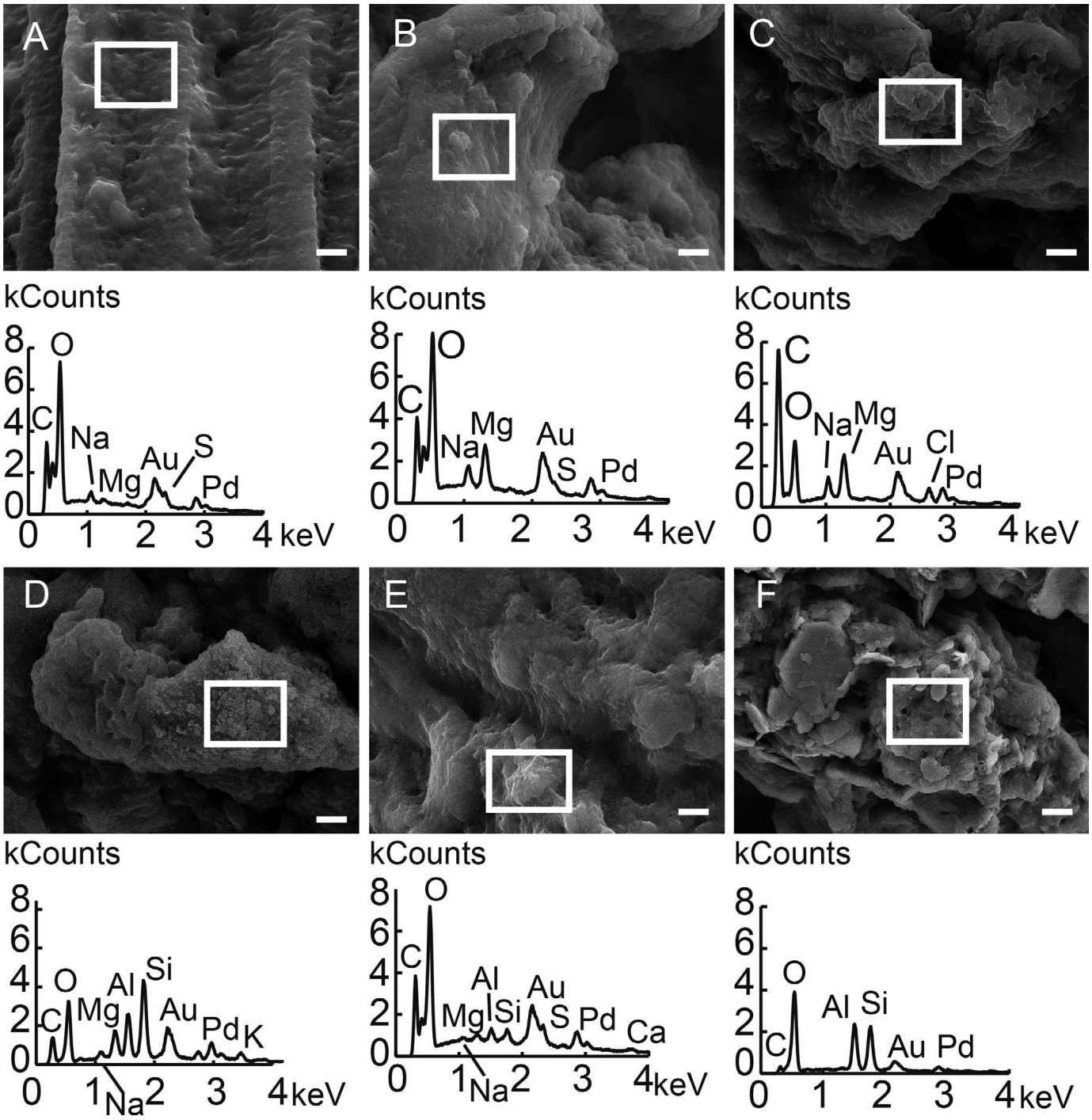

FIG. 3.—Representative scanning electron micrographs and energy dispersive X-ray spectra of scallop muscles exhumed after 45 days of burial (unless otherwise stated). **A**) Muscle tissue on day 0 and before incubation. **B**) Muscle exhumed from quartz sand in the absence of cyanobacteria or added clay minerals. **C**) Muscle exhumed from quartz sand in the presence of cyanobacterial cells. **D**) Muscle exhumed from a substrate containing quartz sand and illite. **E**) Muscle exhumed from kaolinite. Minerals that coat the muscle are fine-grained and morphologically indistinguishable from the organic material. **F**) Platy minerals on the surface of a muscle that was exhumed from kaolinite. All samples were coated with gold and palladium. White boxes show areas analyzed by SEM-EDS; the spectra of these areas are found below corresponding SEM images. Scale bar = 1 μm.

and tissues incubated in quartz sand suggests that these were newly precipitated clay minerals.

When the sediments contained cm-thick layers of illite, two muscles were exhumable on day 30 and only one was recovered on day 45 (Table 1, Online Supplemental File Fig. 2B, 2E). Thus, the presence of illite did not notably enhance the preservation of muscles relative to their preservation in sand without illite (Table 1). However, the presence of illite influenced the composition of minerals in the exhumed samples. When the sediments contained sand and cm-thick layers of illite, the muscles were coated by discontinuous clay veneers. These veneers were not visible to the naked

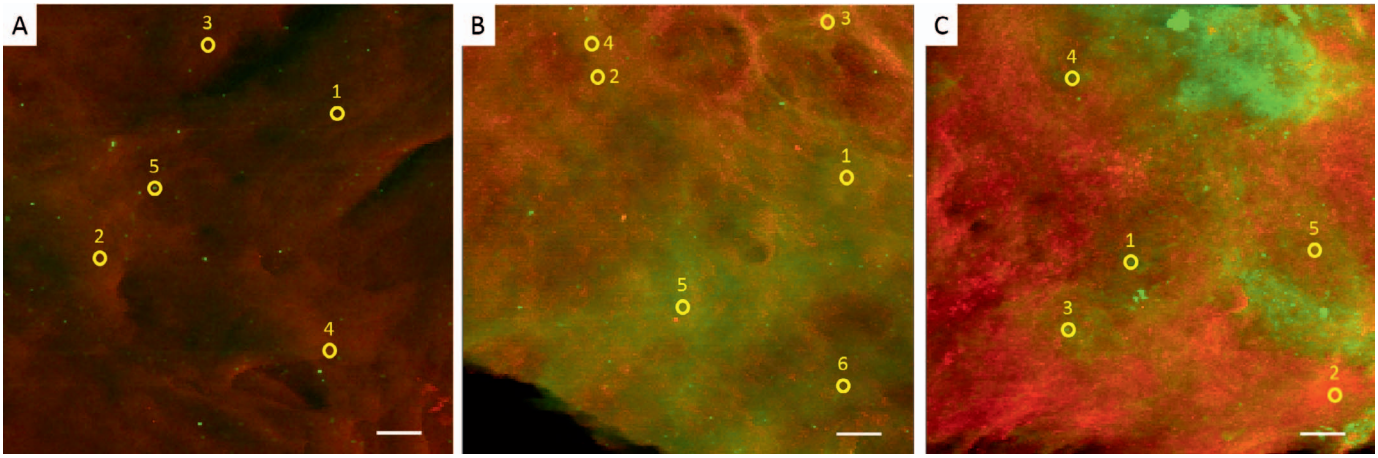

FIG. 4.—Distribution of calcium and iron on muscle surfaces; elemental maps of calcium (red) and iron (green). **A**) Representative muscle before incubation (day 0). **B**) Representative muscle exhumed from quartz sand after 45 days. **C**) Representative muscle exhumed from kaolinite after 45 days. Maps are displayed with the same gamma value of 0.82. The calcium counts scale is 0 to 10660 for all muscle specimens. The iron counts scale is 0 to 5878 for the muscle before experimentation, 0 to 40146 for the muscle exhumed from sand, and 0 to 58778 for the muscle exhumed from kaolinite. Scale bar = 200 μm.

eye (Online Supplemental File Fig. 2B, 2E) and were composed primarily of illite grains that were identical to those in which the muscle was buried (Fig. 3D). We did not sample the porewater for chemical analyses other than pH measurements in this experiment, so we did not calculate mineral saturation indices at different time points.

Porewater Chemistry

Within the first two weeks of muscle burial, the pH of the porewater decreased from 7.6 to 4.5–6.8 in the various replicate experiments (Table 2, Online Supplemental File tables 2, 3). Lower pH values on day 15 were measured around tissues that were incubated in sand or sand with illite relative to kaolinite, where pH values lower than six were never measured even around tissues that underwent complete decay (Online Supplemental File tables 2, 3). Therefore, kaolinite was a more effective buffer of porewater pH than sand. One experiment compared the evolution of additional chemical parameters around muscles buried in sand (three replicate muscles) and those buried in kaolinite (an additional three replicates) (Fig. 6, Online Supplemental File Table 2).

Concentrations of porewater Fe(II) were two or more orders of magnitude higher around decaying tissues compared with the sterile sediments (Online

TABLE 2.—*Saturation indices (SI) for various mineral and other phases on day 15 of muscle burial.*

		Saturation indices					
		Muscles in Sand			Muscles in Kaolinite		
Phase/pH	Chemical formula	R1	R2	R3	R1	R2	R3
Ca-montmorillonite*,[1]	$Ca_{0.165}Al_{2.33}Si_{3.67}O_{10}(OH)_2$	-5.51	2.74	0.92	3.86	3.43	2.32
calcite	$CaCO_3$	-2.62	-0.63	-1.63	-0.62	-0.62	-1.12
chalcedony*	SiO_2	0.65	0.20	0.57	0.50	0.38	0.32
dolomite	$CaMg(CO_3)_2$	-4.43	-0.45	-2.45	-0.44	-0.44	-1.44
ferric hydroxide (a)	$Fe(OH)_3$	1.28	3.65	2.47	3.40	2.02	2.96
iron sulfide (ppt)	FeS	-3.48	-0.20	-0.71	-1.22	-0.43	–
goethite	FeOOH	7.00	9.36	8.19	9.12	7.74	8.67
greigite	Fe_3S_4	13.92	20.76	10.64	–	–	–
hematite	Fe_2O_3	15.98	20.72	18.37	20.22	17.46	19.34
illite*,[1]	$K_{0.6}Mg_{0.25}Al_{2.3}Si_{3.5}O_{10}(OH)_2$	-6.80	2.94	0.32	4.01	3.60	2.13
kaolinite*,[1]	$Al_2Si_2O_5(OH)_4$	-3.00	4.03	2.32	4.64	4.41	3.67
mackinawite	FeS	-2.75	0.54	0.02	-0.49	0.30	–
melanterite	$FeSO_4*7H_2O$	-4.65	-5.53	-4.61	-5.96	-5.57	-5.45
pyrite	FeS_2	15.52	22.97	21.02	21.36	22.55	–
quartz*	SiO_2	1.07	0.62	1.00	0.93	0.81	0.75
siderite	$FeCO_3$	-1.33	-0.22	-0.31	-0.65	-0.29	-0.64
silicon dioxide (a)*	SiO_2	-0.21	-0.66	-0.28	-0.35	-0.47	-0.53
pH	–	4.5	6.5	5.5	6.5	6.5	6.0

Note: Positive values indicate saturation; negative values indicate undersaturation. Dashed lines indicate conditions not favorable for the formation of the given phase. *a* = amorphous phase; *ppt* = precipitate. Solubility constants (*Ks*) were obtained from the computer program PHREEQC Version 1.6.

* SI values were calculated using dissolved silica concentrations from day 20 of muscle burial.

[1] We did not measure aluminum concentrations in the pore fluids and used an assumed value of 0.1 μM (Mackin and Aller 1986). Calculated SI values at aluminum concentrations of 0.01 uM are lower than those shown in the table by 2 to 3 units.

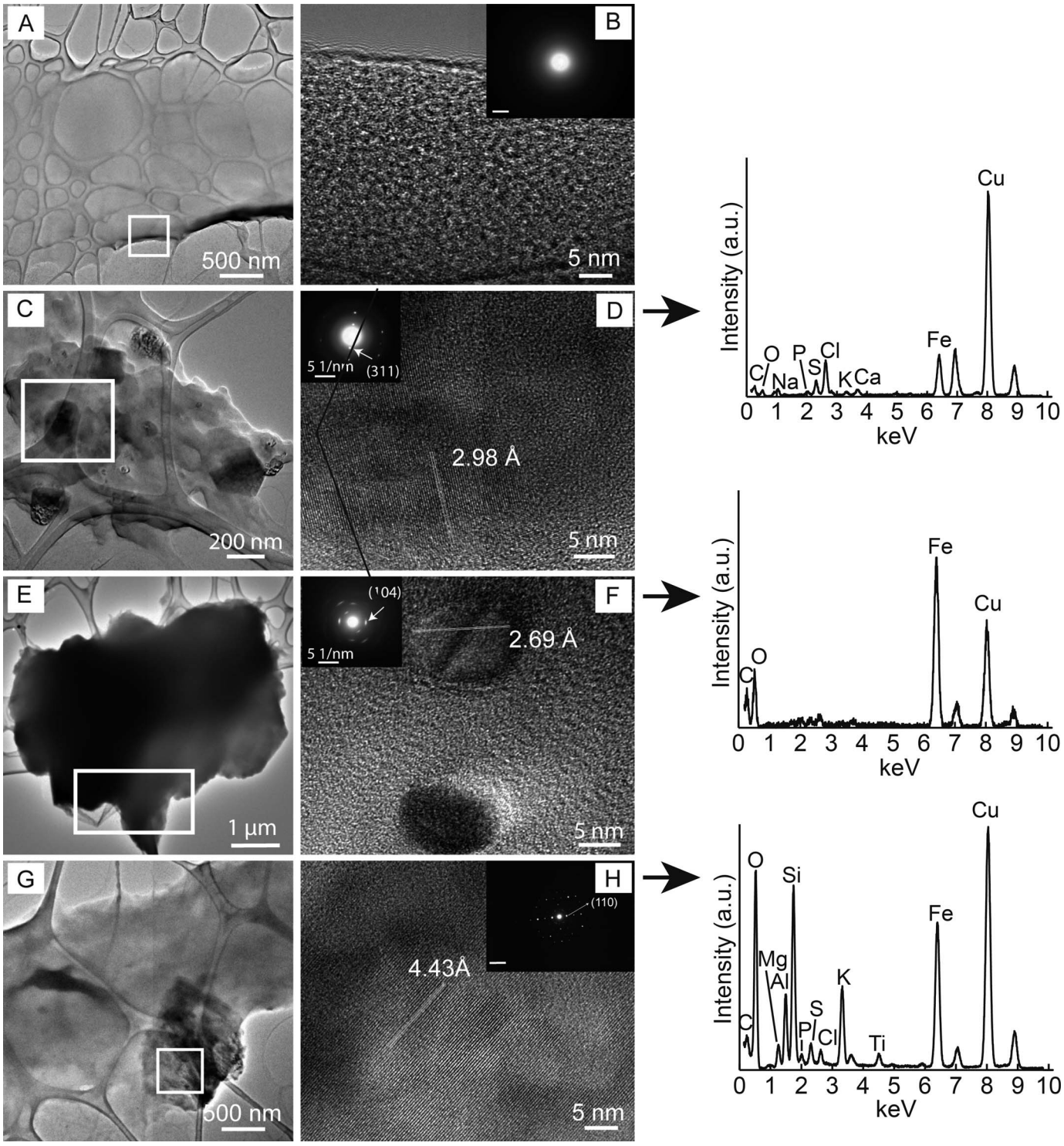

FIG. 5.—TEM-SAED analysis of muscles before and after incubation in kaolinite and quartz sand. **A**) Bright-field transmission electron micrograph (TEM) of muscle before burial. This muscle had no visible dark patches or mineralized areas. **B**) High resolution (HRTEM) image of the tissue area marked in panel A shows the absence of crystalline or microcrystalline minerals. **C**) Muscle exhumed from quartz sand after 45 days. **D**) HRTEM image of the area selected in panel C; diffraction patterns reveal the presence of greigite associated with the soft tissues. **E**) Muscle exhumed from quartz sand after 45 days. The tissue is encrusted by dark minerals. **F**) HRTEM image of the area selected in panel E, showing the presence of hematite. **G**) Muscle exhumed from kaolinite after 45 days of incubation. Tissue is visibly encrusted by minerals. **H**) HRTEM image of the area selected in panel G. Uniform lattice fringe has an interplanar spacing of 4.43 Å. The SAED of the same material shows a diffraction pattern of a crystallite with a monoclinic net pattern of (110) superstructure reflection characteristic of Fe- and K- rich clay minerals (smectite). EDS spectra are shown to the right of corresponding HRTEM images and diffraction patterns.

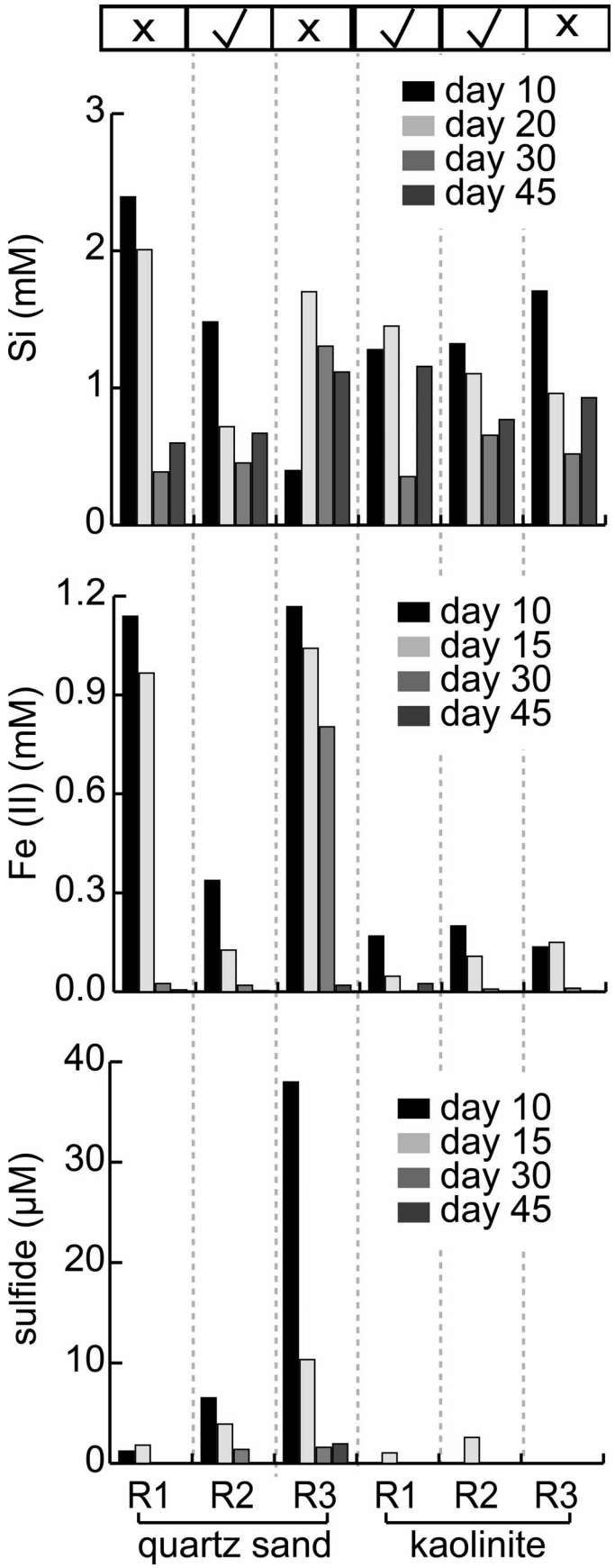

Supplemental File Table 2), indicating the presence of organic electron donors for the microbial reduction of Fe(III) due to muscle decay. In fact, the highest concentrations of Fe(II) were measured in the porewaters around muscles incubated in sand that had lost the greatest amount of mass due to decay (Fig. 6, Online Supplemental File Table 2). The microbial reduction of iron requires both organic electron donors and soluble or solid sources of Fe(III). $FeCl_3$ that was added to the sterile medium before experimentation (see Methods) was one such source. Iron oxides present in the sand were additional sources of Fe(III) (Online Supplemental File methods, Fig. 4A). In contrast, kaolinite standards, including the clay used in the current study, contain mineral impurities, but are unlikely sources of Fe(III) (Online Supplemental File Fig. 4B). In keeping with this, concentrations of Fe(II) were nearly an order of magnitude lower around tissues incubated in kaolinite relative to sand (Fig. 6, Online Supplemental File Table 2). The higher concentrations of soluble Fe(III) around tissues decaying in sand relative to sterile controls (Online Supplemental File Table 2) also suggests that organic decay facilitated the release of soluble Fe(III) from the sand and the oxidation of some reduced Fe(II).

Sulfate reduction in the pore fluids was not limited by the availability of sulfate (5 mM). Sulfide concentrations did not vary in a consistent manner around muscles buried in sand (Fig. 6, Online Supplemental File Table 2), but the calculated saturation indices demonstrated the presence of favorable conditions for the precipitation of greigite during the first 15 days of muscle burial in all sandy pore fluids (Table 2). Sulfide concentrations were lower in kaolinite (Fig. 6, Online Supplemental File Table 2) and the pore fluids were undersaturated with respect to the precipitation of greigite (Table 2). All pore fluids containing muscle tissues were undersaturated with respect to the precipitation of carbonate minerals and sulfates and saturated with respect to the precipitation of iron oxide and hydroxide minerals, such as hematite, goethite, and ferric hydroxide (Table 2). With the exception of a single sand replicate, in which the tissues decayed quickly, pore fluids were also oversaturated with respect to the precipitation of Ca-montmorillonite, illite, and kaolinite. The saturation indices with respect to various clay minerals were higher in porewaters around tissues buried in kaolinite than tissues buried in sand (Table 2), indicating the potential for the precipitation of new clay minerals in the presence of abundant kaolinite.

Organic decay also enabled the mobilization of silica from kaolinite and quartz grains (Fig 6, Online Supplemental File Table 2). The initial medium was undersaturated with respect to the precipitation of amorphous silica (0.1 mM of silica in the initial medium, see Methods), but within weeks, porewater concentrations of silica reached millimolar concentrations (Fig. 6, Online Supplemental File Table 2) and pore fluids were saturated with respect to chalcedony (SiO_2) (Table 2). Replicates in which silica concentrations reached or exceeded 1.5 mM after 10 or 20 days did not contain exhumable muscles at the end of the experiment (Fig. 6, Online Supplemental File Table 2). Moreover, even though the porewaters around muscles contained higher concentrations of dissolved silica relative to the sterile medium and sterile control experiments (Online Supplemental File table 2), we did not observe any evidence for silica cements around exhumed muscles.

DISCUSSION

30-Day Window of Delayed Decay

Preliminary stages of fossilization require some, but not extensive decay (Briggs and Kear 1993, 1994; Briggs 2003; Purnell et al. 2018). Thus, a window of time must exist within which extensive decay and the complete

←

FIG. 6.—Concentrations of dissolved silica, Fe(II), and sulfide in the porewaters around muscles incubated in quartz sand or kaolinite. R1-R3 indicates replicate experiments. Key: X = complete decay of muscle tissue; check mark = muscle was exhumed after 45 days.

deterioration of the macroscopic organism is prevented. Our combined observations suggest that the initial window that determines whether muscle tissues will decay or become preserved does not exceed 30 days. Containers with muscles that lost less than 50% of their initial mass after 30 days consistently yielded exhumable samples on day 45 (Table 1). In contrast, when muscles lost more than 90% of their initial mass by day 30, complete liquefaction/decay of the remaining tissues was observed on day 45 (Table 1). Observables that tracked rampant decay included high concentrations of Fe(II)/dissolved silica (>1 mM) (Fig. 6, Online Supplemental File Table 2) and the formation of black patches around muscles buried in sand (Fig. 2, Online Supplemental File Fig. 2). These patches are commonly found around decaying tissues (e.g., Briggs and Kear 1993; Darroch et al. 2012; Wilson and Butterfield 2014; Naimark et al. 2016a; Gibson et al. 2018) and are likely composed of organic residues and iron sulfide phases (see Naimark et al. 2016a) that are not attached to the muscle surfaces and do not inhibit tissue decay. When these observables were present during the first 15–30 days of tissue burial (Online Supplemental File Table 2), we were unable to exhume muscles on day 45. This suggests that delayed decay and the precipitation of shape-preserving mineral veneers during the first month of incubation are critical for the preservation of muscle tissues, though in natural environments, soft tissues may undergo different rates of decay relative to those in laboratory settings. Moreover, variability in muscle recovery between replicate incubations (Table 1) likely resulted from differences in the endogenous microbiomes of the muscle tissues. Therefore, heterotrophic community compositions and initial concentrations of endogenous bacteria may also affect the window of time required for the exceptional preservation of soft tissues.

Three-Dimensional Preservation of Muscles by Iron Sulfide and Iron Oxide Minerals that Form in Mixed Redox Environments

Iron sulfides are hypothesized to form as early mineral phases around soft tissues buried in coarse-grained sediments (Gehling 1999; Liu 2016). However, fossils of exceptionally preserved soft-bodied organisms more commonly contain iron oxides, which are interpreted to be the products of pyrite oxidation (e.g., Gehling 1999; Mapstone and McIlroy 2006). Thus, direct evidence for the formation of iron sulfides during the early stages of soft tissue burial is often lacking. Our experiments reveal the formation of both iron (II, III) sulfides and iron oxides within muscle tissues during early burial in coarse-grained siliciclastic sediments and indicate that the delayed decay of animal soft tissues can occur under mixed redox conditions. These conditions are expected in environments that are continuously flushed with oxic seawater, such as intertidal and subtidal marine settings (e.g., Bosak et al. 2013). However, delayed decay is much less likely in the presence of mechanical disturbances and redox changes introduced by extensive vertical burrowing during the later Phanerozoic (Seilacher and Pflüger 1994; Tarhan and Droser 2014).

In the current study, the drawdown in porewater pH during the first weeks of muscle decay was greater in sand relative to kaolinite (Online Supplemental File tables 2, 3), likely because the dissolution of quartz sand did not buffer pH as effectively as the dissolution of kaolinite. This, combined with the weekly medium exchange that brought anoxic porewaters into contact with oxic artificial seawater, may have promoted the formation of greigite in muscles incubated in sand. Previous experimental work has shown that greigite can be synthesized under acidic conditions, as a result of reactions involving amorphous iron monosulfide and hydrogen sulfide (e.g., Wada 1977; Rickard 1969). Similar findings have been observed in freshwater and nearshore environments, where greigite formation predominates over competing mineral reactions (e.g., mackinawite/pyrite formation) due to localized acidity and seasonal changes in sediment oxygenation (Hilton et al. 1986; Cutter and Velinsky et al. 1988; Hilton 1990). Thus, heterotrophic decay of the muscle tissues, which dictated the pH and oxygen concentrations of the pore fluids, may have also determined the composition of initial precipitates.

We also suggest that iron sulfides and oxides preserve the exterior of the muscles, while the interior continues to decay (Fig. 7A–7D). This may explain why external features (e.g., Gehling 1999; Callow and Brasier 2009) and the molds of interior surfaces (e.g., Gehling et al. 2000; Tarhan et al. 2015; Bobrovskiy et al. 2019) of soft-bodied organisms are commonly and exceptionally preserved in the fossil record. However, interior details, such as organs and guts, are rarely reported.

Two-Dimensional Preservation of Muscles by Clay Minerals in Kaolinite-Rich Environments

Kaolinite has been shown to inhibit the growth of the aerobic heterotrophic decomposer, *P. luteoviolacea* (McMahon et al. 2016) and the metabolic activities of other microorganisms, such as iron and sulfate reducing bacteria (e.g., Wong et al. 2004). Therefore, the antibacterial properties of kaolinite can explain the lower concentrations of Fe(II) and sulfide measured in kaolinite relative to quartz sand (Fig. 6, Online Supplemental File Table 2). Moreover, dissolved silica that was released due to organic decay and the acidic conditions around muscle tissues, likely facilitated the precipitation of authigenic aluminosilicates around muscles incubated in kaolinite. In the absence of conditions that favor the precipitation of greigite (Table 2), aluminosilicates could form.

Our experiments suggest that delayed decay is associated with the limited activity of sulfate reducing microbes in the presence of mM sulfate concentrations, but also reveal that the availability of iron for microbial iron reduction may be even more critical in the preservation of soft tissues than the previously hypothesized availability of sulfate (Gabbott et al. 2001; Gaines et al. 2012). This is consistent with the reported formation of authigenic Fe(II)-rich clay minerals around diatom frustules in modern suboxic and anoxic, but not sulfidic, silty sediments of the Amazon delta and the suggested role of microbial iron reduction in this process (Michalopoulos and Aller 2004). Our experiments show that authigenic clay minerals can form not only around small siliceous organisms in modern clay-rich deltaic systems, but also around macroscopic and labile animal tissues. A similar mechanism of fossilization in sulfate-poor environments has been proposed for organic-walled fossils of the 1000 Ma Torridon Group of Northwest Scotland (Wacey et al. 2014).

Illite is commonly associated with well-preserved soft-bodied fossils in the rock record, but its occurrence is often attributed to diagenesis (e.g., Gabbott et al. 2001). The surfaces of muscles incubated in the current experiment in the presence of cm-thick layers of illite were coated by discontinuous clay veneers composed primarily of illite grains identical to those from the sediment substrate (Fig. 3D). Because only the top of the muscle was in physical contact with the layer of illite (see Methods), a continuous veneer composed of clay particles did not form around the entire muscle, leaving large areas of tissue exposed to heterotrophic decay. This suggests, at least in our experiments, that illite does not facilitate the formation of continuous mineral veneers and thus, may not be critical to the preservation of soft tissues. However, confirmation of this result depends on experiments that examine the decay of muscle tissues buried in cm-thick layers of illite and sediments with varying amounts of kaolinite, illite, and other clay minerals.

Current observations inspire the following model for the preservation of muscle tissues in kaolinite-rich sediments: (1) during the first days to weeks of tissue burial, kaolinite grains from the sediment adhere to the organic surfaces and form a discontinuous veneer around the muscle tissue; (2) decay of some carbonaceous, but mostly proteinaceous

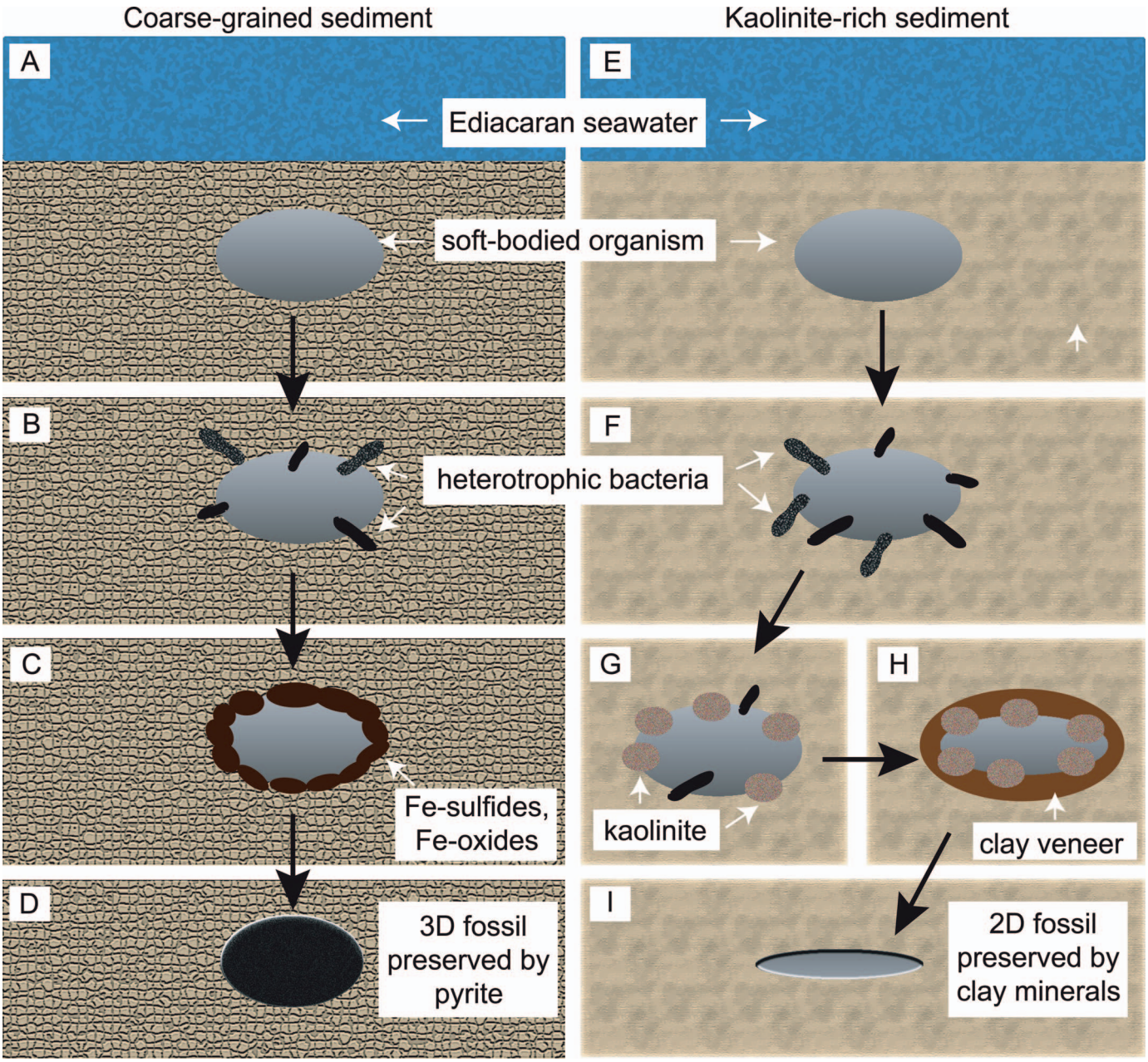

FIG. 7.—Cartoon schematic for the fossilization of muscle tissues in coarse-grained and kaolinite-rich sediments. **A**) Soft-bodied organism is buried in coarse-grained siliciclastic sediment. **B**) Heterotrophic bacteria degrade labile tissues during early burial. **C**) The release of iron and sulfide during heterotrophic decay facilitates the formation of iron sulfides and iron oxides on tissue surfaces. This slows down, but does not prevent, heterotrophic decay and replicates the tissues. **D**) Although this initial decay hinders the preservation of internal features, due to the preferential degradation of nitrogenous compounds, the original thickness of the tissue is preserved and a 3D fossil is formed. **E**) Soft-bodied organism is buried in kaolinite-rich sediment. **F**) Heterotrophic bacteria preferentially degrade proteins and other nitrogenous components. **G**) Kaolinite grains adhere to the soft tissue and form a discontinuous veneer. **H**) The release of iron, silica, and aluminum during decay facilitates the precipitation of authigenic clay minerals and the formation of a continuous veneer around the tissue. This physical barrier slows down the decay and protects organic matter close to the veneers. **I**) The organic matter in the interior decays and the structure becomes vertically compressed due to sediment compaction and additional diagenetic conditions. This leads to the formation of compression fossils.

compounds, during the first month of burial facilitates the formation of anaerobic conditions around the muscles and the release of Si, Fe, and Al into the surrounding porewaters; (3) this process enables the formation of authigenic, cation-rich clay mineral veneers on the surfaces of the decaying tissues. These veneers form a physical barrier that slows down microbially catalyzed decay and preserves the shape of the organism despite continued decay of the interior that leads to the decrease in height. The width, length, and discoidal morphology of the original tissue are preserved, promoting the formation of compression fossils (Fig. 7E–7I). This model is consistent with the reported enrichments of kaolinite or its inferred diagenetic products in event beds that preserve some Burgess Shale-style compression fossils (Forchielli et al. 2014; Anderson et al. 2018).

Comparison to Previous Fossilization Models and Implications for the Siliciclastic Rock Record

Our experiments show that the fossilization of labile muscle tissues in siliciclastic environments depends on biological and environmental factors that enable the formation of authigenic clay minerals, pyrite precursor minerals, and iron oxides. Macroscopic organisms can undergo delayed decay in the absence of sealing surface layers of photosynthetic mats (Gehling 1999), carbonaceous cements (Gaines et al. 2012) or complete porewater anoxia (Gehling 1999; Callow and Brasier 2009).

The current study does not address the preservation potential of recalcitrant cuticles that are commonly preserved as carbonaceous compressions in early Cambrian shales (e.g., Orr et al. 1998; Gaines et al. 2008, 2012). Our model shows that the mineralogy of the sediment that buries organisms strongly controls the type of authigenic minerals formed during delayed decay and may explain the contrasting styles of fossilization of assumed recalcitrant tissues reported in the Ediacaran siliciclastic record. In particular, the eight-armed Ediacaran fossil, *Eoandromeda octobrachiata*, which is thought to have had a recalcitrant exterior, is preserved as carbonaceous compressions in the Doushantou Formation shale in South China, but as casts and molds in the Rawnsley Quartzite sandstone beds of South Australia (Zhu et al. 2008). Moreover, the observed thinness of mineral veneers around experimentally fossilized muscle tissues in the current experiment (Fig. 5) indicates that the detection of similar features in the fossil record may require high-resolution analytical techniques such as TEM and μXRD. In fact, if the veneers are sufficiently thin, the residual carbonaceous material in the fossil compressions may be more easily detected than any compositional differences between the fossil exterior and the surrounding sediment.

The diverse styles of soft tissue fossilization, including both two-dimensional versus three-dimensional preservation and the mineral composition of veneers that form around tissues during early burial may depend on a variety of factors, including biological ones inherent to the organism undergoing preservation and the environment in which the organism lived. Thus, future investigations of varying tissue types, organismal morphologies (discoidal, tubular, etc.), taxonomic groups (annelids, cnidarians, arthropods, etc.), and depositional environment/sediment compositions will be necessary to better constrain factors that enabled the fossilization of soft-bodied Ediacaran organisms in coarse-grained and clay-rich siliciclastic sediments.

CONCLUSION

Our study demonstrates the formation of <10 μm authigenic minerals on the surfaces of muscle tissues incubated in siliciclastic sediments for 45 days in the presence of mixed redox conditions. This occurs in the absence of sealing cyanobacterial mats, but requires active heterotrophic decay, including moderately active microbial iron reduction. Active decay also inhibits the growth of cyanobacterial mats on sediment surfaces, but the type of sediment controls the microbial activity, the extent of tissue decay, and pH changes. Changes in pH and the type of sediment also influence the dissolution of minerals and types of authigenic minerals that form. The low pH in quartz sand enables the formation of iron sulfide and iron oxide minerals. When undecayed, tissues in quartz sand retain their vertical thickness. The burial of muscles in kaolinite is accompanied by smaller pH changes and a smaller extent of microbial iron and sulfate reduction. Tissues preserved in kaolinite develop clay-rich veneers and are vertically compacted. These findings provide evidence for microbial metabolisms and processes that delay the decay of macroscopic soft tissues in siliciclastic sediments.

ACKNOWLEDGMENTS

We acknowledge the members of the Bosak laboratory (MIT) and thank Timothy Cavanaugh (Harvard CNS), Yong Zhang, and Shiahn Chen (MIT CMSE) for their assistance with electron microscopy, Charles Settens (MIT CMSE) and Nobumichi Tamura (ALS) for their help with XRD analyses, and Armeen Taeb (Caltech) for statistical consultation. SBP thanks Robert Gaines (Pomona College) for helpful conversations. We also thank Nicholas Tosca (Oxford), Lidya Tarhan (Yale) and one anonymous reviewer, as well as PALAIOS co-editor Martin Zuschin and associate editor Shuhai Xiao for their thoughtful comments and suggestions on the manuscript. This work was funded by the NASA Astrobiology Institute grant (NNA13AA90A) and grants from the Simons Foundation (327126 and 344707 to TB) and the American Chemical Society Petroleum Research Fund (PRF# 54498-ND8 to TB). MP's work was supported by funding by the NSF FESD Type I: The Dynamics of Earth System Oxygenation project (#1338810), the Templeton Foundation and the Professor Amar G. Bose Research Grant Program, MIT. CNS, a member of the National Nanotechnology Coordinated Infrastructure Network (NNCI), is supported by the National Science Foundation (Award No. 1541959). The operations at the ALS are supported by the Director, Office of Science and Office of Basic Energy Sciences of the U.S. Department of Energy at LBNL under Contract No. DE-AC02-05CH11231.

SUPPLEMENTAL MATERIAL

Data are available from the PALAIOS Data Archive: https://www.sepm.org/supplemental-materials.

REFERENCES

Anderson, E.P., Schiffbauer, J.D., and Xiao, S., 2011, Taphonomic study of Ediacaran organic-walled fossils confirms the importance of clay minerals and pyrite in Burgess Shale-type preservation: Geology, v. 39, p. 643–646, doi: 10.1130/G31969.1.

Anderson, R.P., Tosca, N.J., Gaines, R.R., Koch, N.M., and Briggs, D.E.G., 2018, A mineralogical signature for Burgess Shale-type fossilization: Geology, v. 46, p. 347–350, doi: 10.1130/G39941.1.

Arrouy, M.J., Warren, L.V., Quaglio, F., Poiré, D.G., Simões, M.G., Rosa, M.B., and Peral, L.E.G., 2016, Ediacaran discs from South America: probable soft-bodied macrofossils unlock the paleogeography of the Clymene Ocean: Scientific Reports, v. 6, 30590, doi: 10.1038/srep30590. http://dx.doi.org/10.1038/srep30590.

Berner, R.A., 1969, Migration of iron and sulfur within anaerobic sediments during early diagenesis: American Journal of Science, v. 267, p. 19–42.

Bobrovskiy, I., Krasnova, A., Ivantsov, A., Serezhnikova, E.L., and Brocks, J.J., 2019, Simple sediment rheology explains the Ediacara biota preservation: Nature Ecology and Evolution, v. 3, p. 582–598, doi: 10.1038/s41559-019-0820-7.

Borkow, P.S. and Babcock, L.E., 2003, Turning pyrite concretions outside-in: role of biofilms in pyritization of fossils: The Sedimentary Record, v. 1, p. 4–7.

Bosak, T., Knoll, A.H., and Petroff, A.P., 2013, The meaning of stromatolites: Annual Review of Earth and Planetary Sciences, v. 41, p. 3.1–3.24, doi: 10.1146/annurev-earth-042711-105327.

Briggs, D.E.G., 2003, The role of decay and mineralization in the preservation of soft-bodied fossils: Annual Review of Earth and Planetary Sciences, v. 31, p. 275–301, doi: 10.1146/annurev.earth.31.100901.144746.

Briggs, D.E.G. and Kear, A.J., 1993, Decay and preservation of polychaetes: taphonomic thresholds in soft-bodied organisms: Paleobiology, v. 19, p. 107–135, doi: 10.1017/S0094837300012343.

Briggs, D.E.G. and Kear, A.J., 1994, Decay and mineralization of shrimps: PALAIOS, v. 9, p. 431–456, doi: 10.2307/3515135.

Brindley, G.W. and Sempels, R.E., 1977, Preparation and properties of some hydroxy-aluminum beidellites: Clay Minerals, v. 12, p. 229–237.

Brock, F., Parkes, R.J., and Briggs, D.E.G., 2006, Experimental pyrite formation associated with decay of plant material: PALAIOS, v. 21, p. 499–506, doi: 10.2110/palo.2005.P05-077R.

Bykova, N., Gill, B.C., Grazhdankin, D., Rogov, V., and Xiao, S., 2017, A geochemical study of the Ediacaran discoidal fossil *Aspidella* preserved in limestones: implications for its taphonomy and paleoecology: Geobiology, v. 15, p. 572–587, doi: 10.1111/gbi.12240.

Cai, Y., Hua, H., Xiao, S., Schiffbauer, J.D., and Li, P., 2010, Biostratinomy of the late Ediacaran pyritized Gaojiashan Lagerstätte from southern Shaanxi, South China: importance of event deposits: PALAIOS, v. 25, p. 487–506, doi: 10.2110/palo.2009.p09-133r.

Cai, Y., Schiffbauer, J.D., Hua, H., and Xiao, S., 2011, Morphology and paleoecology of the late Ediacaran tubular fossil *Conotubus hemiannulatus* from the Gaojiashan Lagerstätte of southern Shaanxi Province, South China: Precambrian Research, v. 191, p. 46–57, doi: 10.1016/j.precamres.2011.09.002.

Cai, Y., Schiffbauer, J.D., Hua, H., and Xiao, S., 2012, Preservational modes in the Ediacaran Gaojiashan Lagerstätte: pyritization, aluminosilicification, and carbonaceous

compression: Palaeogeography, Palaeoclimatology, Palaeoecology, v. 326–328, p. 109–117, doi: 10.1016/j.palaeo.2012.02.009.

Callow, R.H.T. and Brasier, M.D., 2009, Remarkable preservation of microbial mats in Neoproterozoic siliciclastic settings: implications for Ediacaran taphonomic models: Earth-Science Reviews, v. 96, p. 207–219, doi: 10.1016/j.earscirev.2009.07.002.

Cutter, G.A. and Velinsky, D.J., 1988, Temporal variations of sedimentary sulfur in a Delaware salt marsh: Marine Chemistry, v. 23, p. 311–327.

Darroch, S.A.F., Boag, T.H., Racicot, R.A., Tweedt, S., Mason, S.J., Erwin, D.H., and Laflamme, M., 2016, A mixed Ediacaran-metazoan assemblage from the Zaris sub-basin, Namibia: Palaeogeography, Palaeoclimatology, Palaeoecology, v. 459, p. 198–208, doi: 10.1016/j.palaeo.2016.07.003.

Darroch, S.A.F., Laflamme, M., Schiffbauer, J.D., and Briggs, D.E.G., 2012, Experimental formation of a microbial death mask: PALAIOS, v. 27, p. 293–303, doi: 10.2110/palo.2011.p11-059r.

Dzik, J., 1999, Organic membranous skeleton of the Precambrian metazoans from Namibia: Geology, v. 27, p. 519–522, doi: 10.1130/0091-7613(1999)027<0519:OMSOTP>2.3.CO;2.

Elliott, D.A., Trusler, P.W., Narbonne, G.M., Vickers-Rich, P., Morton, N., Hall, M., Hoffman, K.H., and Schneider, G.I.C., 2016, *Ernietta* from the late Ediacaran Nama Group, Namibia: Journal of Palaeontology, v. 90, p. 1017–1026, doi: 10.1017/jpa.2016.94.

Erwin, D.H., Laflamme, M., Tweedt, S.M., Sperling, E.A., Pisani, D., and Peterson, K.J., 2011, The Cambrian conundrum: early divergence and later ecological success in the early history of animals: Science, v. 334, p. 1091–1097, doi: 10.1126/science.1206375.

Fedonkin, M.A. and Waggoner, B.M., 1997, The late Precambrian fossil *Kimberella* is a mollusc-like bilaterian organism: Nature, v. 388, p. 868–871, doi: 10.1038/42242.

Forchielli, A., Steiner, M., Kasbohm, J., Hu, S., and Keupp, H., 2014, Taphonomic traits of clay-hosted early Cambrian Burgess Shale-type fossil Lagerstätten in South China: Palaeogeography, Palaeoclimatology, Palaeoecology, v. 398, p. 59–85, doi: 10.1016/j.palaeo.2013.08.001.

Gabbott, S.E., Norry, M.J., Aldridge, R.J., and Theron, J.N., 2001, Preservation of fossils in clay minerals; a unique example from the Upper Ordovician Soom Shale, South Africa: Proceedings of the Yorkshire Geological Society, v. 53, p. 237–244, doi: 10.1144/pygs.53.3.237.

Gaines, R.R., Briggs, D.E.G., and Yuanlong, Z., 2008, Cambrian Burgess Shale-type deposits share a common mode of fossilization: Geology, v. 36, p. 755–758, doi: 10.1130/G24961A.1.

Gaines, R.R., Hammarlund, E.U., Hou, X., Qi, C., Gabbot, S.E., Zhao, Y., Peng, J., and Canfield, D.E., 2012, Mechanisms for Burgess Shale-type preservation: Proceedings of the National Academy of Sciences, v. 109, p. 5180–5184, doi: 10.1073/pnas.1.

Gehling, J.G., 1999, Microbial mats in terminal Proterozoic siliciclastics: Ediacaran death masks: PALAIOS, v. 14, p. 40–57, doi: 10.2307/3515360.

Gehling, J.G., Narbone, G.M., and Anderson, M.M., 2000, The first named Ediacaran body fossil, *Aspidella terranovica*: Paleontology, v. 43, p. 427–456.

Gehling, J.G. and Vickers-Rich, P., 2007, The Ediacara Hills, *in* M.A. Fedonkin, J.G. Gehling, K. Grey, G.M. Narbonne, and P. Vickers-Rich (eds.), The Rise of Animals: The Johns Hopkins University Press, Baltimore, MD, p. 89–114.

Gibson, B.M., Schiffbauer, J.D., and Darroch, S.A.F., 2018, Ediacaran-style decay experiments using mollusks and sea anemones: PALAIOS, v. 33, p. 185–203.

Griffin, J.J., Windom, H., and Goldberg, E.D., 1968, The distribution of clay minerals in the World Ocean: Deep-Sea Research, v. 15, p. 433–459, doi: 10.1016/0011-7471(68)90051-X.

Grimes, S.T., Brock, F., Rickard, D., Davies, K.L., Edwards, D., Briggs, D.E.G., and Parkes, R.J., 2001, Understanding fossilization: experimental pyritization of plants: Geology, v. 29, p. 123–126, doi: 10.1130/0091-7613(2001)029<0123:UFEPOP>2.0.CO;2.

Hilton, J., 1990, Greigite and the magnetic properties of sediments: Limnology and Oceanography, v. 35, p. 509–520, doi: 10.4319/lo.1990.35.2.0509.

Hilton, J., Lishman, J.P., and Chapman, J.S., 1986, Magnetic and chemical characterisation of a diagenetic magnetic mineral formed in the sediments of productive lakes: Chemical Geology, v. 56, p. 325–333, doi: 10.1016/0009-2541(86)90012-4.

Laflamme, M., Schiffbauer, J.D., Narbonne, G.M., and Briggs, D.E.G., 2011, Microbial biofilms and the preservation of the Ediacara biota: Lethaia, v. 44, p. 203–213, doi: 10.1111/j.1502-3931.2010.00235.x.

Liu, A.G., 2016, Framboidal pyrite shroud confirms the 'death mask' model for moldic preservation of Ediacaran soft-bodied organisms: PALAIOS, v. 31, p. 259–274, doi: 10.2110/palo.2015.095.

Liu, A.G., McMahon, S., Matthews, J.J., Still, J.W., and Brasier, A.T., 2019, Petrological evidence supports the death mask model for the preservation of Ediacaran soft-bodied organisms in South Australia: Geology, v. 47, p. 215–218, doi: 10.1130/G45918.1.

Locatelli, E.R., McMahon, S., and Bilger, H., 2017, Biofilms mediate the preservation of leaf adpression fossils by clays: PALAIOS, v. 32, p. 708–724, doi: 10.2110/palo.2017.043.

Mackin, J.E. and Aller, R.C., 1986, The effects of clay mineral reactions on dissolved Al distributions in sediments and waters of the Amazon continental shelf: Continental Shelf Research, v. 6, p. 245–262, doi: 10.1016/0278-4343(86)90063-4.

Mapstone, N.B. and McIlroy, D., 2006, Ediacaran fossil preservation: taphonomy and diagenesis of a discoid biota from the Amadeus Basin, central Australia: Precambrian Research, v. 149, p. 126–148, doi: 10.1016/j.precamres.2006.05.007.

Marcus, M.A., MacDowell, A.A., Celestre, R., Manceau, A., Miller, T., Padmore, H.A., and Sublett, R.E., 2004, Beamline 10.3.2 at ALS: a hard X-ray microprobe for environmental and materials sciences: Journal of Synchrotron Radiation, v. 11, p. 239–247, doi: 10.1107/S0909049504005837.

Martin, D., Briggs, D.E.G., and Parkes, R.J., 2004, Experimental attachment of sediment particles to invertebrate eggs and the preservation of soft-bodied fossils: Journal of the Geological Society, v. 161, p. 735–738, doi: 10.1144/0016-764903-164.

McMahon, S., Anderson, R.P., Saupe, E.E., and Briggs, D.E.G., 2016, Experimental evidence that clay inhibits bacterial decomposers: implications for preservation of organic fossils: Geology, v. 44, p. 867–870, doi: 10.1130/G38454.1.

Meyer, M., Elliott, D., Schiffbauer, J.D., Hall, M., Hoffman, K.H., Schneider, G., Vickers-Rich, P., and Xiao, S., 2014a, Taphonomy of the Ediacaran fossil *Pteridinium simplex* preserved three-dimensionally in mass flow deposits, Nama Group, Namibia: Journal of Paleontology, v. 88, p. 240–252, doi: 10.1666/13-047.

Meyer, M., Elliott, D., Wood, A.D., Polys, N.F., Colbert, M., Maisano, J.A., Vickers-Rich, P., Hall, M., Hoffman, K.H., Schneider, G., and Xiao, S., 2014b, Three-dimensional microCT analysis of the Ediacara fossil *Pteridinium simplex* sheds new light on its ecology and phylogenetic affinity: Precambrian Research, v. 249, p. 79–87, doi: 10.1016/j.precamres.2014.04.013.

Michalopoulos, P. and Aller, R.C., 2004, Early diagenesis of biogenic silica in the Amazon delta: alteration, authigenic clay formation, and storage: Geochimica et Cosmochimica Acta, v. 68, p. 1061–1085, doi: 10.1016/j.gca.2003.07.018.

Naimark, E., Kalinina, M., and Boeva, N., 2018a, Persistence of external anatomy of small crustaceans in a long term taphonomic experiment: PALAIOS, v. 33, p. 154–163, doi: 10.2110/palo.2017.083.

Naimark, E., Kalinina, M., Shokurov, A., Boeva, N., Markov, A., and Zaytseva, L., 2016a, Decaying in different clays: implications for soft-tissue preservation: Palaeontology, v. 59, p. 583–595, doi: 10.1111/pala.12246.

Naimark, E.B., Kalinina, M.A., Shokurov, A.V., Markov, A.V., and Boeva, N.M., 2016b, Decaying of *Artemia salina* in clay colloids: 14-month experimental formation of subfossils: Journal of Paleontology, v. 90, p. 472–484, doi: 10.1017/jpa.2016.23.

Naimark, E., Kalinina, M., Shokurov, A., Markov, A., Zaytseva, L., and Boeva, N., 2018b, Mineral composition of host sediments influences the fossilization of soft tissues: Canadian Journal of Earth Sciences, v. 55, p. 1271–1283, doi: 10.1139/cjes-2017-0237.

Narbonne, G.M., 2005, The Ediacara biota: Neoproterozoic origin of animals and their ecosystems: Annual Review of Earth and Planetary Sciences, v. 33, p. 421–442, doi: 10.1146/annurev.earth.33.092203.122519.

Newman, S.A., Klepac-Ceraj, V., Mariotti, G., Pruss, S.B., Watson, N., and Bosak, T., 2017, Experimental fossilization of mat-forming cyanobacteria in coarse-grained siliciclastic sediments: Geobiology, v. 15, p. 484–498, doi: 10.1111/gbi.12229.

Newman, S.A., Mariotti, G., Pruss, S., and Bosak, T., 2016, Insights into cyanobacterial fossilization in Ediacaran siliciclastic environments: Geology, v. 44, p. 579–582, doi: 10.1130/G37791.1.

Orr, P.J., Briggs, D.E.G., and Kearns, S.L., 1998, Cambrian Burgess Shale animals replicated in clay minerals: Science, v. 281, p. 1173–1175, doi: 10.1126/science.281.5380.1173.

Pajusalu, M., Borlina, C.S., Seager, S., Ono, S., and Bosak, T., 2018, Open-source sensor for measuring oxygen partial pressures below 100 microbars: PLoS ONE, v. 13, e0206678, doi: 10.1371/journal.pone.0206678.

Petrovich, R., 2001, Mechanisms of fossilization of the soft-bodied and lightly armored faunas of the Burgess Shale and of some other classical localities: American Journal of Science, v. 301, p. 683–726, doi: 10.2475/ajs.301.8.683.

Pilson, M.E.Q., 2013, An Introduction to the Chemistry of the Sea: Cambridge University Press, New York, NY, 524 p.

Purnell, M.A., Donoghue, P.J.C., Gabbott, S.E., McNamara, M.E., Murdock, D.J.E., and Sansom, R.S., 2018, Experimental analysis of soft-tissue fossilization: opening the black box: Palaeontology, v. 61, p. 317–323, doi: 10.1111/pala.12360.

Rickard, D.T., 1969, The chemistry of iron sulphide formation at low temperatures: Stockholm Contributions in Geology, v. 20, p. 67–95.

Schiffbauer, J.D., Xiao, S., Cai, Y., Wallace, A.F., Hua, H., Hunter, J., Xu, H., Peng, Y., and Kaufman, A.J., 2014, A unifying model for Neoproterozoic–Palaeozoic exceptional fossil preservation through pyritization and carbonaceous compression: Nature Communications, v. 5, 5754, doi: 10.1038/ncomms6754.

Seilacher, A. and Pflüger, F., 1994, From biomats to benthic agriculture: a biohistoric revolution, *in* W.E. Krumbein, D.M. Paterson, and L.J. Stal (eds.), Biostabilization of Sediments: Bibliotheks - und Informationssystem der Universitat Oldenburg, Oldenburg, Germany, p. 97–105.

Smith, E.F., Nelson, L.L., Strange, M.A., Eyster, A.E., Rowland, S.M., Schrag, D.P., and Macdonald, F.A., 2016, The end of the Ediacaran: two new exceptionally preserved body fossil assemblages from Mount Dunfee, Nevada, USA: Geology, v. 44, p. 911–914, doi: 10.1130/G38157.1.

Smith, E.F., Nelson, L.L., Tweedt, S.M., Zeng, H., and Workman, J.B., 2017, A cosmopolitan late Ediacaran biotic assemblage: new fossils from Nevada and Namibia support a global biostratigraphic link: Proceedings of the Royal Society B, v. 284, 20170934, doi: 10.1098/rspb.2017.0934.

Tarhan, L.G. and Droser, M.L., 2014, Widespread delayed mixing in early to middle Cambrian marine shelfal settings: Palaeogeography, Palaeoclimatology, Palaeoecology, v. 399, p. 310–322, doi: 10.1016/j.palaeo.2014.01.024.

Tarhan, L.G., Droser, M.L., and Gehling, J.G., 2015, Depositional and preservational environments of the Ediacara Member, Rawnsley Quartzite (South Australia): assessment of paleoenvironmental proxies and the timing of 'ferruginization': Palaeogeography, Palaeoclimatology, Palaeoecology, v. 434, p. 4–13, doi: 10.1016/j.palaeo.2015.04.026.

Tarhan, L.G., Hood, A.v.S., Droser, M.L., Gehling, J.G., and Briggs, D.E.G., 2016, Exceptional preservation of soft-bodied Ediacara Biota promoted by silica-rich oceans: Geology, v. 44, p. 951–954, doi: 10.1130/G38542.1.

Tarhan, L.G., Planavsky, N.J., Wang, X., Bellefroid, E.J., Droser, M.L., and Gehling, J.G., 2018, The late-stage "ferruginization" of the Ediacara Member (Rawnsley Quartzite, South Australia): insights from uranium isotopes: Geobiology, v. 16, p. 35–48, doi: 10.1111/gbi.12262.

Wacey, D., Saunders, M., Roberts, M., Menon, S., Green, L., Kong, C., Culwick, T., Strother, P., and Brasier, M.D., 2014, Enhanced cellular preservation by clay minerals in 1 billion-year-old lakes: Scientific Reports, v. 4, 5841, doi: 10.1038/srep05841.

Wada, H., 1977, The synthesis of greigite from a polysulfide solution at about 100°C: Bulletin of the Chemical Society of Japan, v. 50, p. 2615–2617.

Wilson, L.A. and Butterfield, N.J., 2014, Sediment effects on the preservation of Burgess Shale-type compression fossils: PALAIOS, v. 29, p. 145–154, doi: 10.2110/palo.2013.075.

Wong, D., Suflita, J.M., McKinley, J.P., and Krumholz, L.R., 2004, Impact of clay minerals on sulfate-reducing activity in aquifers: Microbial Ecology, v. 47, p. 80–86, doi: 10.1007/s00248-003-1021-z.

Xiao, S. and Laflamme, M., 2009, On the eve of animal radiation: phylogeny, ecology and evolution of the Ediacara biota: Trends in Ecology and Evolution, v. 24, p. 31–40, doi: 10.1016/j.tree.2008.07.015.

Zhu, M., Gehling, J.G., Xiao, S., Zhao, Y., and Droser, M.L., 2008, Eight-armed Ediacara fossil preserved in contrasting taphonomic windows from China and Australia: Geology, v. 36, p. 867–870, doi: 10.1130/G25203A.1.

Received 28 March 2019; accepted 12 August 2019.